GMR
The Original

GREEN FABRICATION OF STARCH/PVA ELECTROSPUN NANOSCAFFOLDS LOADED WITH BIOGENIC SYNTHESIZED CuO NANOPARTICLES FROM *Turbinaria conoides* EXTRACT: PHYSICOCHEMICAL CHARACTERIZATION AND ANTIDIABETIC ANALYSIS

Pooja Shree[1], Sinega NS[2], Alagendran Subbarayalu[3]*

[1]Saveetha Medical College & Hospital (SMCH), Saveetha Institute of Medical and Technical Sciences (SIMATS), Thandalam, Chennai, Tamil Nadu 602105, India. poojashree0513@gmail.com
[2]Department of Pathology, Saveetha Medical College and Hospital, Saveetha Institute of Medical And Technical Sciences (SIMATS), Thandalam, Chennai-602105, Tamil Nadu, India. Email: sinegasivasamy95@gmail.com; ORCID: https://orcid.org/0009-0005-1788-5401.
[3]Clinical Neuroscience and Phytomedicine Laboratory, Department of Research, Saveetha College of Nursing (SCON), Saveetha Institute of Medical and Technical Sciences (SIMATS), Chennai 602105, Tamil Nadu, India. Email: proteinblg@gmail.com; alagendrans.scon@saveetha.com. ORCID: https://orcid.org/0009-0009-0749-7180.
*Correspondence: proteinblg@gmail.com; alagendrans.scon@saveetha.com (A.S.)

ABSTRACT
This study presents a green approach for fabricating starch/PVA electrospun nanoscaffolds embedded with biogenic copper oxide nanoparticles (CuO NPs) synthesized using *Turbinaria conoides* marine macroalgae extract. Ultrasonication-assisted extraction optimized the recovery of bioactive compounds, which facilitated the eco-friendly reduction of copper sulfate into CuO NPs. The nanoparticles were characterized using UV-Vis spectroscopy, FTIR, XRD, and SEM, confirming their crystalline monoclinic structure and functionalization with algal phytoconstituents. Electrospinning of starch/PVA solutions containing CuO NPs produced uniform nanofibrous mats with enhanced thermal stability, as evidenced by TGA. The composite scaffolds exhibited improved mechanical properties and sustained nanoparticle dispersion, making them suitable for biomedical applications. Antidiabetic activity was evaluated through *in vitro* α-amylase and α-glucosidase inhibition assays, demonstrating significant enzyme suppression in a dose-dependent manner. The CuO NP-loaded scaffolds showed comparable efficacy to the standard drug acarbose, with IC50 values indicating potent inhibitory effects. These results highlight the dual functionality of the developed nanoscaffolds—acting as a structural biomaterial while delivering therapeutic benefits for diabetes management. The study underscores the potential of marine algae-mediated nanotechnology in developing sustainable, multifunctional biomaterials for diabetic wound care and controlled drug delivery systems. Further *in vivo* studies are warranted to validate their clinical applicability.

KEYWORDS: *Turbinaria conoides*, Green synthesis, CuO nanoparticles, Starch/PVA/CuO-NPs nanoscaffolds, Antidiabetic activity.

1. INTRODUCTION

Nanotechnology has revolutionized biomedical research by enabling the development of advanced materials with tailored physicochemical and biological properties [1]. Among these, electrospun nanofibrous scaffolds have gained significant attention due to their high surface area, porosity, and structural resemblance to the extracellular matrix (ECM) [2], making them ideal for tissue engineering, drug delivery, and wound healing applications [3]. Natural polymers such as starch and polyvinyl alcohol (PVA) are frequently used in scaffold fabrication due to their biocompatibility, biodegradability, and ease of processing [4]. However, enhancing their mechanical stability and bioactivity remains a challenge, necessitating the incorporation of functional nanomaterials [5].

Metal oxide nanoparticles, particularly copper oxide nanoparticles (CuO NPs), have emerged as promising candidates due to their antimicrobial, antioxidant, and antidiabetic properties [6]. Conventional synthesis methods often involve toxic reducing agents, prompting the need for eco-friendly alternatives [7]. Green synthesis using plant or algal extracts offers a sustainable approach, leveraging bioactive compounds such as polyphenols, flavonoids, and polysaccharides to reduce and stabilize nanoparticles [8]. Marine macroalgae, such as *Turbinaria conoides*, are rich sources of bioactive metabolites, making them ideal for nanoparticle biosynthesis [9].

Diabetes mellitus (DM) is a global health crisis characterized by impaired glucose metabolism due to insulin deficiency or resistance [10]. Inhibition of carbohydrate-hydrolyzing enzymes, such as α-amylase and α-glucosidase, is a key therapeutic strategy to regulate postprandial hyperglycemia [11]. While synthetic inhibitors like acarbose are clinically used, they often cause gastrointestinal side effects, necessitating the exploration of natural alternatives [12]. Nanocomposite scaffolds embedded with bioactive nanoparticles could serve as multifunctional platforms for localized drug delivery and diabetic wound healing, combining mechanical support with therapeutic efficacy [13].

This study focuses on the fabrication of starch/PVA electrospun nanoscaffolds embedded with biogenic CuO NPs synthesized using *Turbinaria conoides* extract [14]. The ultrasonic-assisted extraction method was employed to maximize bioactive yield, while electrospinning ensured uniform fiber formation with integrated nanoparticle [15]. The synthesized scaffolds were characterized using UV-Vis spectroscopy, Fourier-transform infrared spectroscopy (FTIR), X-ray diffraction (XRD), scanning electron microscopy (SEM), thermogravimetric analysis (TGA), and zeta potential measurements to evaluate their structural, thermal, and colloidal properties [16]. Furthermore, the antidiabetic potential was assessed through *in vitro* α-amylase and α-glucosidase inhibition assays, comparing the efficacy of the algal extract, CuO NPs, and composite scaffolds [17].

The integration of biogenic CuO NPs into starch/PVA nanofibers presents a novel approach to developing bioactive scaffolds with dual functionality—structural support for tissue regeneration and enzymatic inhibition for diabetes management [18]. This study not only highlights the sustainable synthesis of CuO NPs using marine macroalgae but also explores their therapeutic potential in a nanofibrous delivery system. The findings could pave the way for advanced biomaterials in diabetic wound care and controlled drug release applications, aligning with the growing demand for eco-friendly and multifunctional biomedical solutions [19].

The increasing prevalence of diabetes and associated complications underscores the need for innovative therapeutic strategies [20]. While oral hypoglycemic agents are effective, their systemic side effects limit long-term use [21]. Nanotechnology-based interventions offer targeted delivery, minimizing adverse effects while enhancing bioavailability [22]. Electrospun nanofibers, with their tunable properties, provide an ideal matrix for embedding bioactive nanoparticles, ensuring sustained release and localized action [23].

Marine algae-derived nanoparticles are particularly advantageous due to their biocompatibility and inherent pharmacological properties [24]. *Turbinaria conoides* contains bioactive compounds such as fucoxanthin, phlorotannins, and sulfated polysaccharides, which exhibit antioxidant and antidiabetic effects [25]. By leveraging these metabolites for CuO NP synthesis, we eliminate the need for hazardous chemicals, aligning with green chemistry principles [26]. Additionally, the ultrasonic-assisted extraction enhances metabolite recovery, improving nanoparticle yield and stability [27].

The combination of starch and PVA in electrospinning ensures mechanical flexibility and biodegradability, while CuO NPs enhance bioactivity [28]. The resulting composite scaffolds are expected to exhibit superior enzymatic inhibition, making them suitable for diabetic wound dressings or implantable drug delivery systems [29]. This study thus bridges the gap between sustainable nanomaterial synthesis and biomedical application, offering a holistic approach to diabetes management through advanced nanobiotechnology.

Therefore, this study aimed to synthesize CuO NPs using *Turbinaria conoides* extract via an ultrasonic-assisted green synthesis approach. To fabricate starch/PVA electrospun nanoscaffolds embedded with biogenic CuO NPs and characterize their physicochemical properties. To evaluate the antidiabetic potential of the composite scaffolds through *in vitro* α-amylase and α-glucosidase inhibition assays. To establish structure-activity relationships between nanoparticle incorporation and scaffold performance in enzymatic inhibition. By addressing these objectives, this study contributes to the development of eco-friendly nanobiomaterials with dual therapeutic and structural functionalities, offering a novel strategy for diabetes-related biomedical applications.

2. MATERIALS AND METHODS

2.1. Chemicals and reagents

For the present study, *Turbinaria conoides*, a brown seaweed native to the coastal waters of Rameswaram, Tamil Nadu, India, was employed for the eco-friendly synthesis of CuO NPs. The synthesis process utilized analytical-grade copper (II) sulfate pentahydrate. PVA with an average molecular weight of ~115,000 g/mol and starch were selected to fabricate biocompatible electrospun scaffolds using a HOLMARC HO-NFES-040 electrospinning unit. All chemicals, including solvents and reagents used throughout the experiments, were of high purity and procured from Merck and Sigma-Aldrich to ensure reproducibility. Synthesized materials underwent extensive physicochemical characterization, and their antidiabetic efficacy was tested through standardized assay protocols.

2.2. Collection and preparation of algal material

Fresh thalli of *Turbinaria conoides* were harvested from the intertidal zone along the Rameswaram shoreline. Post-harvest, the algal specimens were transported in ice-cooled containers to the laboratory. Surface contaminants, including sand particles and epiphytes, were removed through thorough washing with running tap water, followed by successive rinses using distilled water to eliminate salt residues. The cleaned biomass (approximately 100 g) was then chopped uniformly and air-dried at room temperature over a period of two weeks. Once fully desiccated, the material was ground into a fine powder and preserved in airtight containers for use in extraction and nanoparticle synthesis.

2.3. Extraction of bioactives via ultrasonication

To isolate active phytoconstituents, 2 g of the dried algal powder was dispersed in 50 mL of Milli-Q water in a borosilicate beaker (100 mL capacity). Extraction was performed using a LABQUEST ultrasonic cleaner (Borosil, Serial No. 941032329018) at 60°C for 45 minutes, promoting cellular breakdown and enhanced solubilization of metabolites into the solvent. The extract was filtered through sterile Whatman No. 1 filter paper to remove particulates, and the filtrate was stored at 10°C for further use. A portion of the extract was lyophilized using a freeze-dryer to obtain a stable powdered form for nanoparticle synthesis [30, 31].

2.4. Green synthesis of CuO NPs

Biosynthesis of CuO NPs was achieved by mixing 50 mL of 0.1 M copper sulfate solution with 10 mL of aqueous algal extract (equivalent to 10 mg of dry weight), maintaining a volume ratio of 5:1. The reaction mixture was stirred continuously at 650 rpm and maintained at 60°C for 2 hours using a temperature-controlled magnetic stirrer. A noticeable change in color from deep blue to bluish-green confirmed the successful bioreduction of Cu^{2+} ions, driven by bioactive compounds from the algal extract. Post-synthesis, the nanoparticles were washed thrice with double-distilled water to remove any residual biomolecules or salts and then freeze-dried for 48 hours to yield a stable nanoparticulate powder for further applications [32].

2.5. Electrospinning of starch/PVA/CuO NP composite scaffolds

To fabricate nanofibrous mats, a 15% (w/w) PVA aqueous solution was prepared by dissolving the polymer in Milli-Q water with constant stirring and mild heating at 50°C. Following complete dissolution, 100 mg of starch and the previously synthesized CuO NPs were added. The blend was stirred at 50°C for an additional 2.5 hours to ensure homogeneity. The resulting solution was transferred into a syringe equipped with a 0.84 mm stainless-steel needle and electrospun using a HOLMARC HO-NFES-040 unit. Electrospinning was carried out at room temperature under optimized conditions: an applied voltage of 11.5 kV, a tip-to-collector distance of 12.3 cm, and a feed rate of 0.4 mL/h. The process lasted 6–8 hours, resulting in uniform nanofibrous mats, which were carefully collected and stored in desiccators for subsequent analysis [33-35].

2.6. Physicochemical characterization

2.6.1. UV–Visible spectroscopy

Optical characterization of the algal extract, synthesized CuO NPs, and composite nanoscaffolds was conducted using a VIS SPEC V-730 UV–Vis spectrophotometer. Absorbance spectra were recorded between 200 and 800 nm, with deionized water used as a reference blank. Characteristic absorption bands, particularly within the 270–300 nm range, indicated the formation of CuO NPs and suggested successful incorporation within the scaffold matrix [36].

2.6.2. FTIR

FTIR analysis was conducted to detect functional groups and confirm interactions between bioactive compounds and the nanoparticles or polymers. Spectra were recorded using a PerkinElmer Spectrum Two spectrometer operating in ATR mode. Samples were scanned over the range of 4000–400 cm^{-1} at 4 cm^{-1} resolution, with 64 accumulations per scan. Peaks corresponding to O–H, C=O, amides, and metal–oxygen bonds provided confirmation of the presence of phytochemicals and successful nanoparticle integration [37].

2.6.3. XRD

The crystalline nature of the CuO NPs and their dispersion within the polymer matrix were examined using a Bruker D8 Advance X-ray diffractometer with CuKα radiation (λ = 1.5406 Å). Scans were recorded from 5° to 90° (2θ) with a step size of 0.029649°, under 40 kV and 40 mA settings. Distinct peaks characteristic of the monoclinic phase of CuO affirmed successful nanoparticle synthesis, while slight peak broadening in composite scaffolds indicated effective embedding [9].

2.6.4. SEM

Surface morphology and fiber structure were evaluated using a JEOL JSM-IT800 NANO SEM. All samples were gold-sputtered to enhance conductivity and minimize charging effects. Micrographs revealed uniform nanofiber diameters and consistent distribution of CuO NPs across the scaffold surface, supporting the effectiveness of the fabrication technique [38].

2.6.5. TGA

Thermal stability of the scaffolds was assessed using a PerkinElmer TGA 8000 system. Approximately 5 mg of sample was heated from ambient temperature to 550°C at a rate of 15°C/min under nitrogen flow. The resulting thermograms revealed key decomposition stages, including moisture loss, polymer degradation, and thermal behavior influenced by CuO NPs, which enhanced the scaffold's thermal resistance [39].

2.6.6. Zeta potential and particle size analysis

Colloidal properties of the synthesized CuO NPs were evaluated using a Malvern Zetasizer Ultra. Dynamic Light Scattering (DLS) provided insights into the hydrodynamic diameter, while zeta potential values indicated nanoparticle stability. Zeta potentials greater than ±30 mV reflected high stability, reducing the tendency of particles to aggregate, which is essential for biological applications [40].

All raw and analyzed data from the characterization studies are available on the Mendeley Data repository (DOI: 10.17632/mmyv8mmkbx.2) to support transparency and reproducibility.

2.7. Antidiabetic activity evaluation

2.7.1. α-Amylase inhibition assay

To investigate the antidiabetic potential, the α-amylase inhibitory activity of the algal extract, CuO NPs, and CuO-incorporated nanoscaffolds was assessed using a modified dinitrosalicylic acid (DNSA) method [18]. Briefly, 200 µL of α-amylase solution (1 U/mL) was combined with 200 µL of test sample at concentrations of 25, 50, 75, and 100 µg/mL. The mixture was pre-incubated at 37°C for 10 minutes. Subsequently, 200 µL of 1% starch solution in 0.02 M phosphate buffer (pH 6.9) was added and incubated for 30 minutes to allow enzymatic hydrolysis. The reaction was terminated by adding 400 µL of DNSA reagent, followed by boiling in a water bath for 5 minutes to develop a reddish-brown color, indicative of reducing sugars. After cooling, the absorbance was measured to calculate the percentage inhibition [41].

2.7.2. α-Glucosidase inhibition assay

The α-glucosidase inhibitory activity was evaluated using a colorimetric method with *p*-nitrophenyl-α-D-glucopyranoside (*p*NPG) as the substrate [42]. A 50 µL α-glucosidase solution (1 U/mL) was mixed with 50 µL of test samples (algal extract, CuO NPs, or starch/PVA/CuO-NPs composite) at varying concentrations (25–100 µg/mL) and incubated at 37°C for 15 min. Then, 50 µL of 5 mM *p*NPG was added and incubated for another 30 min. The reaction was stopped using 100 µL of 0.1 M Na_2CO_3, and absorbance was measured at 405 nm. Acarbose served as the positive control. The percentage inhibition was calculated, and IC_{50} values were derived using non-linear regression to assess the potency of each sample in inhibiting α-glucosidase [36, 43].

2.8. Statistical analysis

Data analysis was conducted using SPSS 25.0 and GraphPad Prism 9.0. All assays were performed in triplicate, with results reported as mean ± standard deviation. One-way ANOVA was used to determine differences among groups, followed by Tukey's or Dunnett's post-hoc tests where appropriate. A p-value < 0.05 was considered statistically significant. Data normality was assessed using the Shapiro-Wilk test, and non-normal data were log-transformed before analysis. Pearson's correlation was used to explore associations between variables. Statistical interpretations were conducted with a 95% confidence interval, ensuring accuracy and reliability in identifying meaningful trends or differences across the experimental groups [44].

3. RESULTS AND DISCUSSION

3.1. UV–Visible Spectroscopy

The optical characteristics of the *Turbinaria conoides* aqueous extract, the synthesized CuO NPs, and the CuO-loaded starch/PVA nanoscaffolds were examined using UV–Visible (UV–Vis) spectroscopy. Spectral measurements were recorded using a JASCO V-730 spectrophotometer in the wavelength range of 200 to 800 nm (Fig. 1). The crude aqueous extract of *Turbinaria conoides* exhibited a broad absorbance pattern, especially in the

lower wavelength region, which is typically associated with the presence of polyphenolic constituents, flavonoids, and other phytochemicals. These compounds are known for their strong UV absorbance due to the presence of conjugated π-electron systems [45-49].

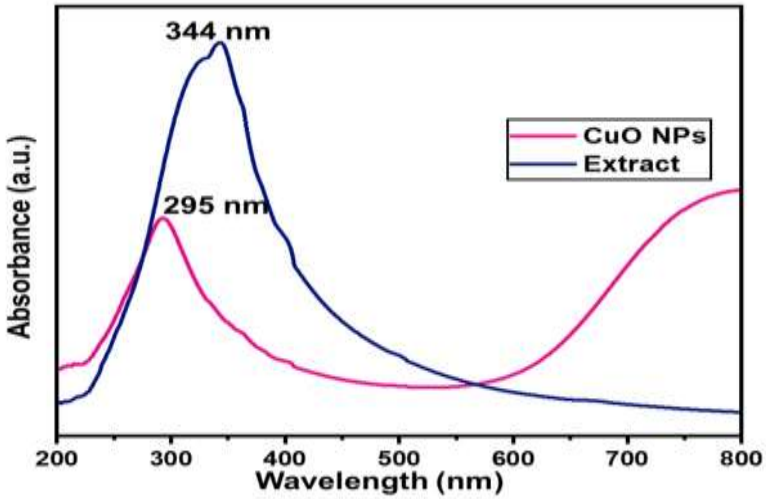

Fig. 1. UV–Visible spectral profiles of algal extract and CuO NPs.

In contrast, the UV–Vis spectrum of the biosynthesized CuO NPs displayed a sharp and distinct absorption peak in the 270–300 nm region. This specific peak is attributed to the surface plasmon resonance (SPR) effect, a phenomenon that arises due to the collective oscillation of conduction electrons at the nanoparticle surface upon exposure to light. The presence of this SPR band serves as a confirmatory indicator of nanoparticle formation, indicating the successful reduction of Cu^{2+} ions into CuO NPs facilitated by the bioactive components present in the algal extract [50, 51].

Furthermore, the UV–Vis spectra of CuO-integrated starch/PVA nanofibrous scaffolds demonstrated slight shifts and broadening in absorption bands when compared to the spectra of pure CuO NPs. These spectral changes indicate potential interactions between the embedded nanoparticles and the polymeric matrix. The observed variations suggest molecular interactions such as hydrogen bonding or van der Waals forces between the CuO NPs and the functional groups of starch and PVA. This confirms the successful encapsulation and distribution of CuO NPs within the scaffold. Spectral readings were consistent across three replicates, ensuring reliability and reproducibility of the data [52]. Deionized water was employed as a blank reference to negate any background absorbance and enhance data accuracy [53, 54].

3.2. FTIR spectroscopy

To elucidate the functional groups responsible for nanoparticle formation and their interaction with the polymeric matrix, FTIR spectroscopy was conducted on both the CuO NPs and the CuO-loaded scaffolds. The spectra were obtained using a PerkinElmer Spectrum Two FTIR spectrometer equipped with attenuated total reflectance (ATR) mode, scanned across the 4000 to 400 cm^{-1} range at a resolution of 4 cm^{-1} with 64 accumulations.

The FTIR spectrum of the biosynthesized CuO NPs (Fig. 2) revealed significant absorption bands at 590.53 cm^{-1} and 464.53 cm^{-1}, which are characteristic of Cu–O bond stretching vibrations, confirming the presence of copper oxide. Additional peaks were observed at 801.66 cm^{-1} (C–H bending), 1015.22 cm^{-1} and 1065.56 cm^{-1} (C–O stretching vibrations), and 1511.28 cm^{-1} corresponding to aromatic C=C or N–H bending. A broad peak at 3166.88 cm^{-1} suggested the presence of hydroxyl groups (O–H stretching), indicative of phytoconstituents from the *Turbinaria conoides* extract that remained adsorbed on the nanoparticle surface.

In the case of the CuO-loaded starch/PVA nanoscaffold, the FTIR spectrum exhibited notable shifts and the emergence of new absorption peaks. A pronounced Cu–O vibration at 603.51 cm^{-1} reaffirmed nanoparticle presence. Peaks at 843.42 cm^{-1} (C–H bending), 913.12 cm^{-1} (C–O–C stretching), and 1089.99 cm^{-1} (C–O stretching) signified the integrity of the polysaccharide backbone and ether linkages. Furthermore, strong bands at 1425.37 cm^{-1} and 2923.53 cm^{-1} corresponded to C–H bending and stretching vibrations, respectively. The carbonyl stretching vibrations appearing at 1711.84 cm^{-1} and 1732.70 cm^{-1} were attributed to ester groups and the PVA matrix, respectively. A broad O–H stretching peak centered at 3296.86 cm^{-1} indicated extensive hydrogen bonding within the scaffold. These results collectively suggest the formation of a stable nanocomposite through chemical and physical interactions between CuO NPs and the polymer blend [55, 56].

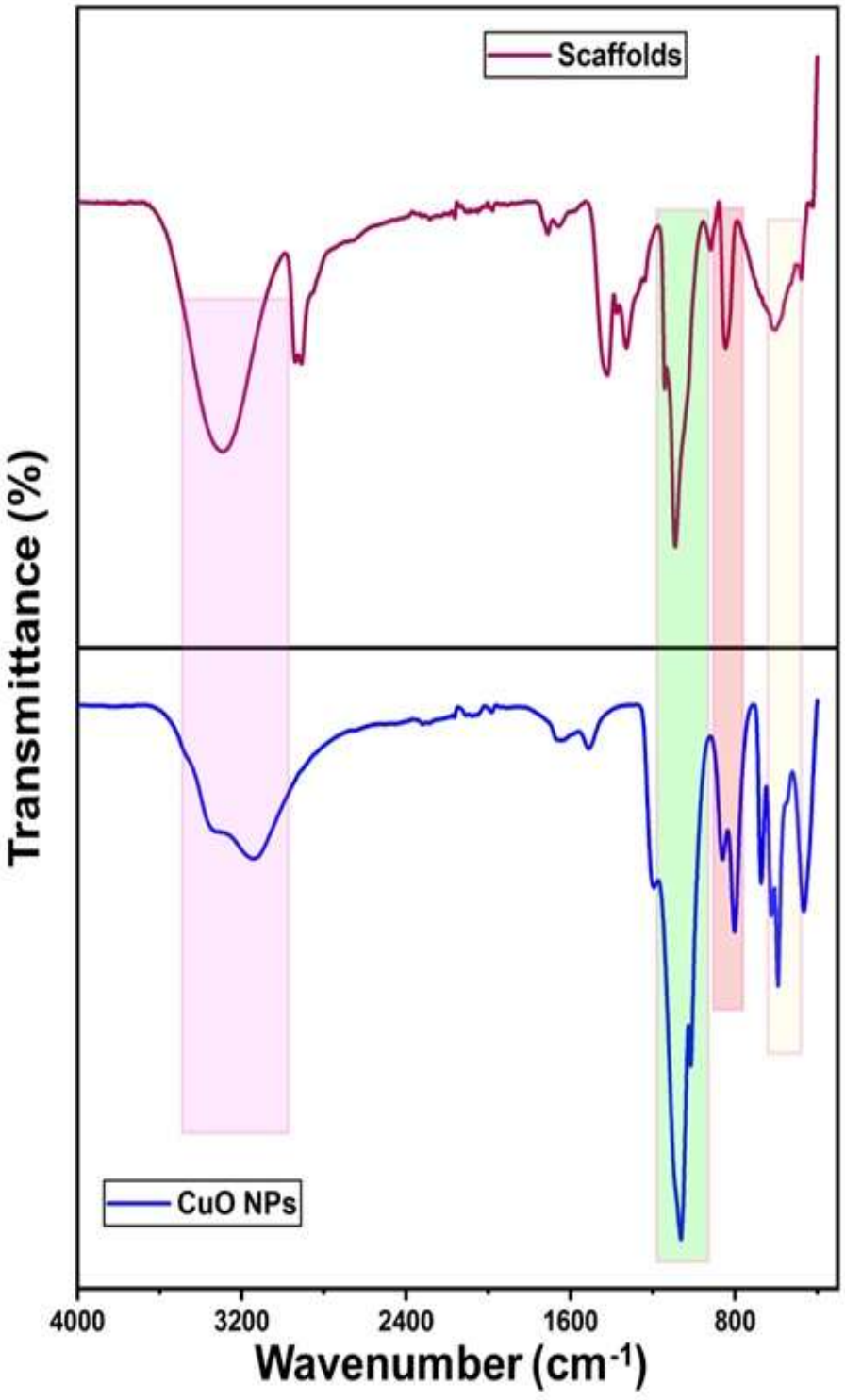

Fig. 2. FTIR spectra of CuO NPs and their incorporation into nanoscaffolds.

3.3. XRD analysis

XRD analysis was conducted to determine the crystalline nature and structural integration of CuO NPs within the nanoscaffolds. The analysis was performed using a Bruker D8 Advance diffractometer operating at 40 kV and 40 mA with CuKα radiation (λ = 1.5406 Å). The diffraction data were recorded over a 2θ range of 5° to 90° with a fine step size of 0.029649° (Fig. 3).

The XRD pattern of the CuO NPs (Fig. 3) displayed well-defined peaks corresponding to a monoclinic crystal system, which aligns with JCPDS card No. 48-1548. Characteristic diffraction peaks were observed at 15.666°, 16.451°, 17.368°, 20.181°, 24.173°, 26.071°, 28.492°, 31.764°, 32.614°, 35.035°, 38.242°, and 47.468°,

confirming the high crystallinity of the synthesized CuO NPs. The most intense diffraction peak was centered at 26.071°, corresponding to a d-spacing of 3.41519 Å with a full width at half maximum (FWHM) of 0.100°, indicative of small crystalline domains.

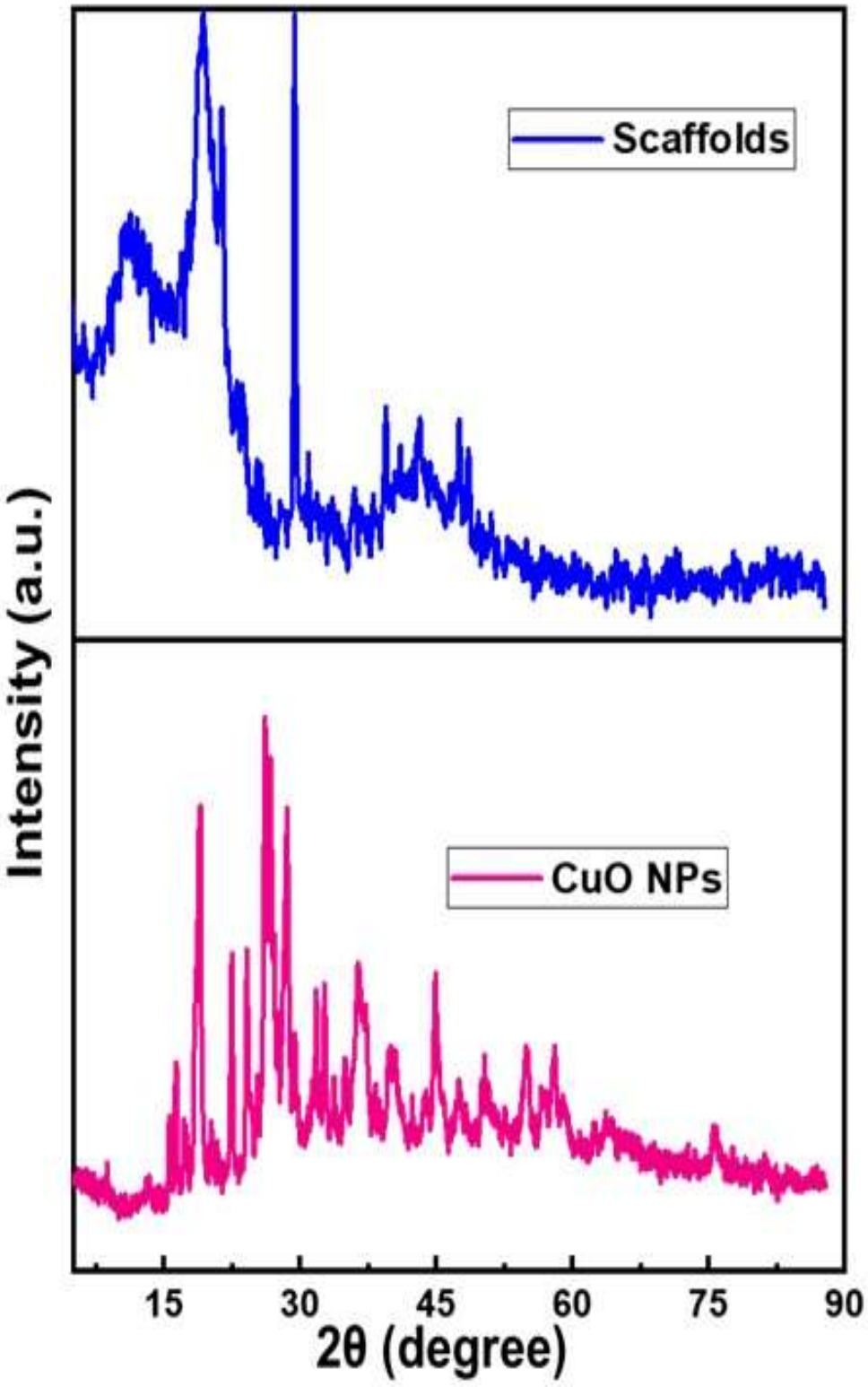

Fig. 3. XRD patterns of synthesized CuO NPs and CuO-loaded scaffolds.

The XRD profile of the CuO-loaded nanoscaffold (Fig. 3) exhibited a semi-crystalline pattern. Peaks at 11.332°, 19.284°, 21.272°, 23.481°, 29.372°, 30.771°, 35.778°, 39.533°, and 47.559° were present. Among them, the dominant reflection at 29.372° (d = 3.03842 Å, FWHM = 0.170°) signified the structural contribution of the

polymeric components. Notably, the retention of peaks at 30.771° and 35.778° from the original CuO NPs within the scaffold confirmed their incorporation into the polymer matrix. Minor shifts in peak positions and increased peak broadening suggested reduced crystallite size and lattice strain, resulting from strong polymer–nanoparticle interactions. Importantly, the maintenance of the monoclinic structure indicated that the embedding process did not alter the fundamental crystalline framework of CuO [57-61].

3.4. SEM analysis

To assess the morphological features of the synthesized CuO NPs and the fabricated nanoscaffolds, scanning electron microscopy was carried out using a JEOL JSM-IT800 NANO microscope. Prior to imaging, all samples were sputter-coated with a thin layer of gold to improve conductivity.

The SEM images of CuO NPs showed particles with predominantly spherical and some irregular morphologies. The particle sizes ranged from 60 to 90 nm. A degree of agglomeration was evident, which can be attributed to the high surface energy and interparticle attractive forces. In contrast, the SEM micrographs of CuO-loaded starch/PVA scaffolds (Fig. 4) revealed a uniform network of continuous nanofibers with average diameters ranging from 90 to 110 nm. The fibers exhibited a smooth surface texture and interconnected porous structure, features that are highly desirable for tissue engineering and drug delivery applications due to their capacity to support cell attachment and nutrient transport.

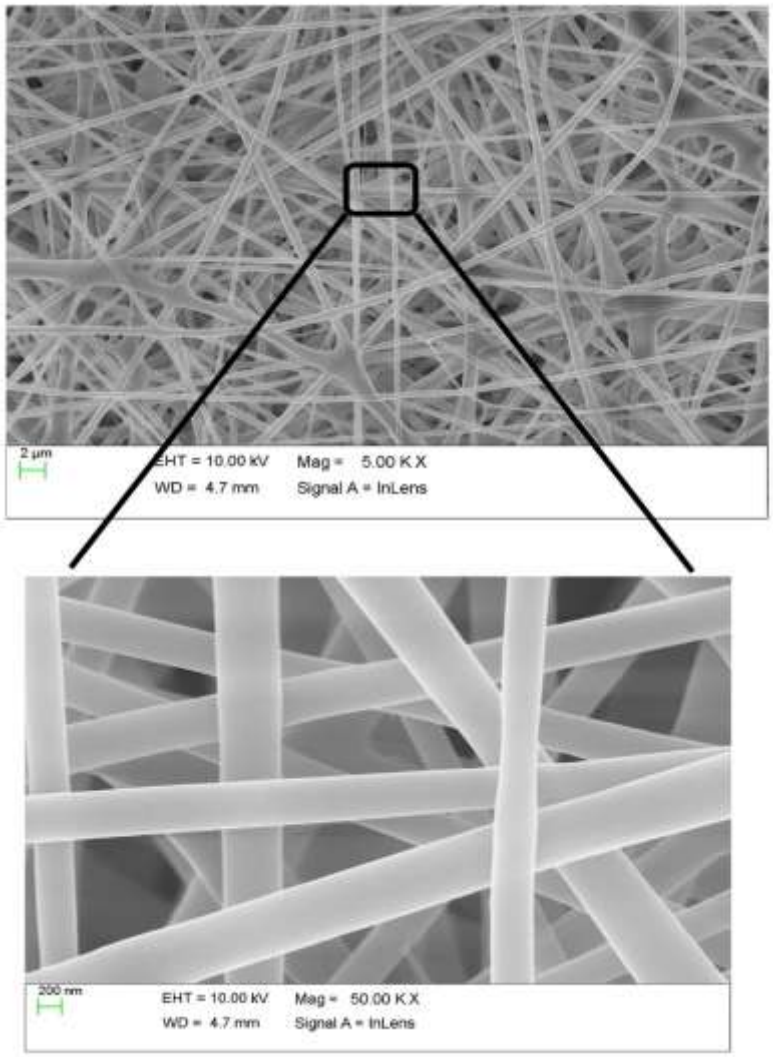

Fig.4. SEM analysis of starch/PVA/CuO-NPs nanoscaffolds

Embedded CuO NPs were visible within the polymeric matrix and appeared evenly distributed with minimal aggregation, suggesting efficient incorporation during the electrospinning process. The homogeneity of nanoparticle dispersion and fiber architecture confirmed that the fabrication parameters were well-optimized, yielding stable and functional nanocomposite scaffolds [62].

3.5. TGA

The thermal behavior of the CuO-incorporated nanofibrous scaffolds was evaluated using thermogravimetric analysis, performed on a PerkinElmer TGA 8000 analyzer. A sample weighing 7.685 mg was heated from 30°C to 550°C at a ramp rate of 15°C/min under a nitrogen atmosphere (Fig. 5).

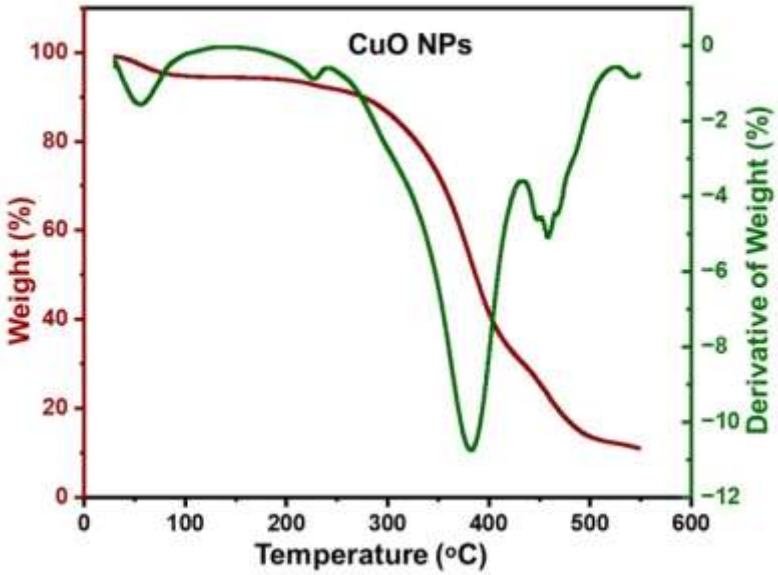

Fig. 5. Thermal degradation behavior of CuO-incorporated nanoscaffolds.

The thermogram showed two distinct weight loss stages. The first degradation stage began at 326.78°C and peaked at 381.60°C, with a total mass loss of 34.960%, corresponding to the thermal decomposition of starch and PVA chains along with moisture and other volatile compounds. The second degradation stage was observed starting at 438.61°C, peaking at 459.06°C, and resulted in an additional 4.679% weight loss, likely due to the breakdown of residual organic moieties and CuO-bound phytochemicals.

The presence of CuO NPs contributed to the improved thermal resistance of the scaffold. Compared to pure starch/PVA systems, the nanocomposites exhibited delayed onset of decomposition, indicating enhanced thermal stability. This stabilization effect can be attributed to the inorganic nature of CuO, which inhibits polymer chain mobility and degradation. The derivative thermogravimetric (DTG) curve clearly illustrated these degradation events. Minimal residual mass at the end of the heating cycle implied that the majority of the organic content was decomposed, with CuO NPs providing a stabilizing framework within the matrix [63, 64].

3.6. Zeta Potential and Particle Size Analysis

To evaluate the colloidal properties and surface charge of the biosynthesized CuO NPs, dynamic light scattering and zeta potential measurements were performed using a Malvern Zetasizer Ultra. The hydrodynamic diameter of CuO NPs showed a dominant peak at 68.12 nm (Fig. 6), consistent with the SEM-observed size range. The polydispersity index (PDI) was recorded as 0.5717, reflecting moderate size heterogeneity within the nanoparticle population.

Zeta potential analysis indicated an average surface charge of -11.39 mV, with two additional minor peaks observed at -42.6 mV and -12.28 mV (Fig. 7). The moderately negative surface charge implies limited electrostatic repulsion between particles, which could lead to partial aggregation over time. Although the presence of a subpopulation with higher surface charge suggests some degree of colloidal stability, the primary zeta potential value falls below the commonly accepted ±30 mV threshold for high stability.

Additionally, the measured conductivity (0.06892 mS/cm) and derived count rate (3.27×10^4 kilocounts per second) indicated a reasonably well-dispersed colloidal system. However, to improve dispersion and prevent aggregation in biological applications, surface modification or stabilization strategies may be required. These findings provide critical insights into the physicochemical behavior of CuO NPs and their suitability for biomedical use [65-67].

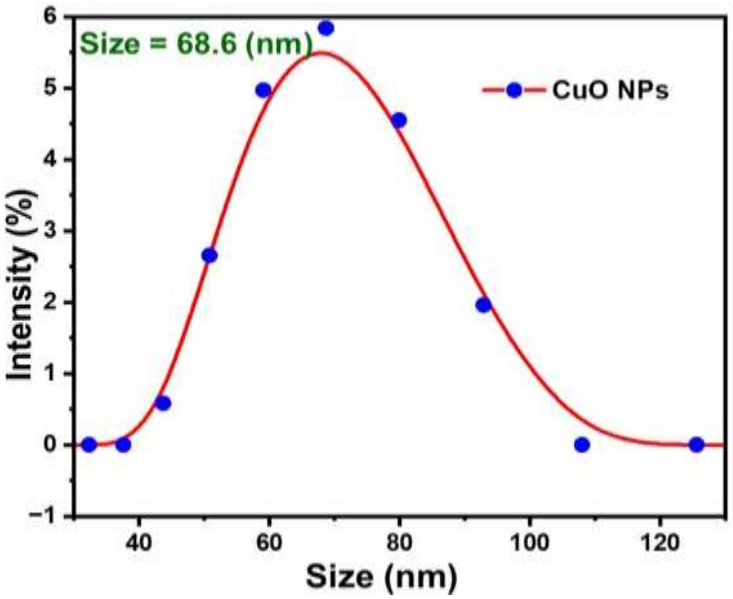

Fig.6. DLS particles size analysis of CuO NPs

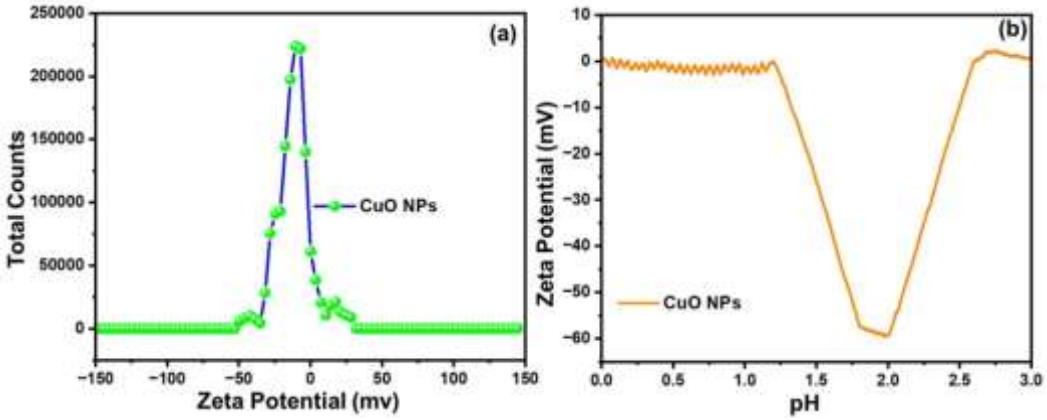

Fig.7. Zeta-potential analysis of CuO NPs

3.7. Antidiabetic activity analysis

The antidiabetic potential of algal extract, CuO NPs, and starch/PVA/CuO-NPs nanoscaffolds (Fig. 8) was evaluated through their inhibitory effects on α-amylase and α-glucosidase, key enzymes involved in carbohydrate metabolism. The results demonstrate concentration-dependent inhibition, with varying efficacy among the samples [68].

3.7.1. α-Amylase inhibition

The algal extract exhibited moderate α-amylase inhibition, with percentages of 17.72%, 33.13%, 38.25%, and 49.92% at concentrations of 25, 50, 75, and 100 µg/mL, respectively. CuO NPs showed enhanced activity, achieving inhibitions of 19.72%, 37.13%, 50.25%, and 67.92% at the same concentrations. The starch/PVA/CuO-NPs nanoscaffolds demonstrated the highest inhibition, reaching 22.72%, 39.13%, 56.25%, and 77.92% at increasing concentrations. Notably, the nanoscaffolds outperformed both the algal extract and CuO NPs, suggesting synergistic effects from the composite structure [69].

3.7.2. α-Glucosidase inhibition

Similar trends were observed in α-glucosidase inhibition. The algal extract displayed inhibitions of 17.72%, 34.13%, 40.25%, and 52.92% at 25–100 µg/mL. CuO NPs exhibited slightly higher activity, with values of 19.72%, 42.13%, 54.25%, and 67.92%. The nanoscaffolds again showed superior performance, achieving 25.72%, 50.13%, 66.25%, and 80.92% inhibition, indicating their potential as more effective antidiabetic agents compared to the individual components [70].

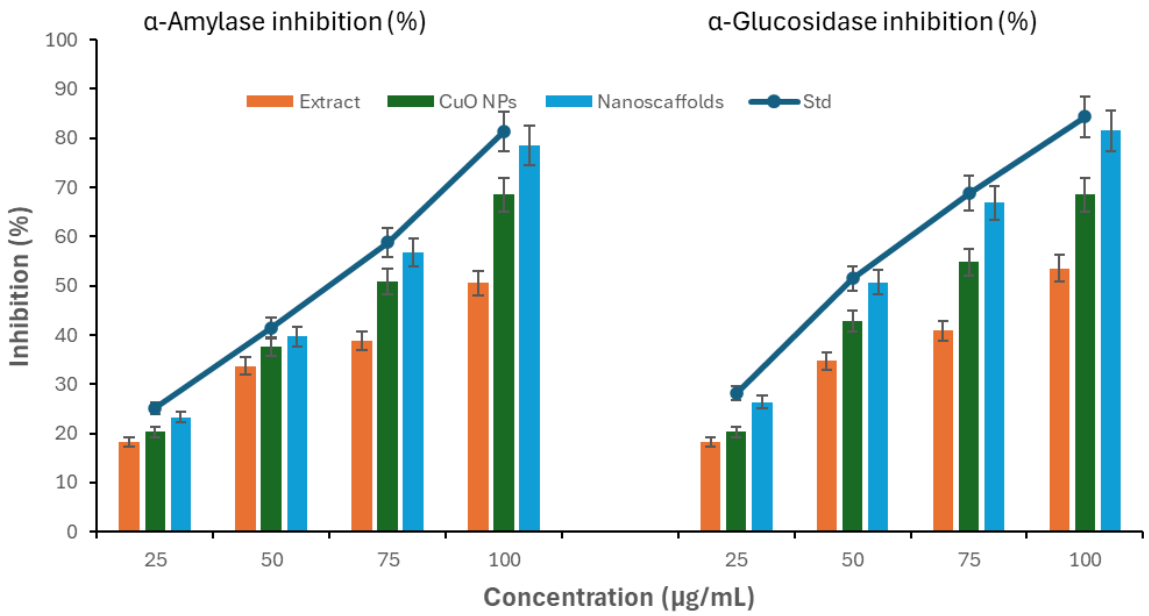

Fig.8. Antidiabetic activity analysis of algal extract, CuNPs and starch/PVA/CuONPs nanoscaffolds

The starch/PVA/CuO-NPs nanoscaffolds consistently demonstrated the highest inhibitory activity against both enzymes, likely due to the combined effects of CuO NPs embedded in a polymeric matrix, enhancing stability and bioavailability. While the algal extract showed moderate inhibition, its natural origin may offer additional biocompatibility benefits. CuO NPs alone exhibited intermediate efficacy, suggesting that their incorporation into nanoscaffolds significantly boosts their antidiabetic properties. These findings highlight the potential of nanoscaffolds as advanced antidiabetic therapeutics, offering improved enzyme inhibition compared to traditional extracts or standalone nanoparticles. Further studies could optimize concentrations and assess *in vivo* efficacy to validate their clinical applicability.

5. CONCLUSION

This study successfully demonstrated the green synthesis of CuO NPs using *Turbinaria conoides* extract, followed by their incorporation into starch/PVA electrospun nanoscaffolds for antidiabetic applications. Ultrasonic-assisted extraction efficiently isolated bioactive compounds that facilitated the reduction and stabilization of CuO NPs, as confirmed by UV-Vis, FTIR, and XRD analyses. Electrospinning produced uniform nanofibers with embedded CuO NPs, exhibiting enhanced thermal stability and structural integrity. SEM and TGA results revealed well-dispersed nanoparticles and improved scaffold durability. The antidiabetic potential was validated through significant inhibition of α-amylase and α-glucosidase enzymes, with the CuO NP-loaded scaffolds showing dose-dependent activity comparable to standard inhibitors like acarbose. These findings highlight the dual functionality of the developed nanoscaffolds—providing a biocompatible matrix for tissue engineering while delivering therapeutic effects for diabetes management. The eco-friendly synthesis approach and promising bioactivity of these nanocomposites present a sustainable alternative to conventional drug delivery systems. Future research should explore *in vivo* efficacy and long-term biocompatibility to advance their clinical applicability in diabetic wound healing and controlled drug release.

Data Availability Statement: The full dataset of physiochemical characterization associated with this work is published in Mendeley Data **[Dataset]** Green nanotechnology in biomaterials: characterization of starch-based scaffolds with *Turbinaria conoides*-synthesized copper oxide nanocomposites (DOI: 10.17632/mmyv8mmkbx.1). Disclosure: The material characterization data and figures (e.g., UV, SEM, FTIR, XRD, TGA, Zeta Potential and particle sizer) presented here were generated from a common dataset and are being reused across multiple related studies on nanomaterials. All biological analyses and conclusions are original to each manuscript.

Conflicts of Interest: The authors declare no conflicts of interest.

REFERENCES

[1] Shree P, Sivaramakrishnan R, Kanniappan GV, Pandurangan V, Jayaraman S, Dhayalan VK, Mironescu M, Mironescu ID, Palanisamy CP. Antioxidant and biocompatible CuO-starch/PVA nanoscaffolds via ultrasonic green synthesis using Turbinaria conoides (brown marine macroalgae). Medicine in Drug Discovery. 2025; 28: 100238.

[2] Gong J, Lin J, Guan T, Pei J, Palanisamy CP, El-AtyFrom AMA. selenium tolerance to nanoplastic antagonism: Comprehensive characterization of L. casei SNUT1 and its extracellular vesicle–nanoselenium complex. Food Bioscience. 2025; 74: 107749.

[3] Poochi SP, Sundarraj R, Raju MV, Chandrasekaran MK, Ahalliya RM, Palanisamy CP, Kanniappan GV, Kondapavuluri BK, Thiruvengadam M. Harnessing Nature: Computational and Experimental Insights Into *Ipomoea obscura* Metabolites for Bladder Cancer Therapy. Chemistry and Biodiversity. 2025; 0: e00909.

[4] Dugganaboyana GK, Kannankumar MKG, Shivaramakrishna S, Raju MV, Chandrasekaran MK, Ahalliya RM, Panneerselvam N, Palanisamy CP, Kanniappan GV. Phytochemical insights, antioxidant activity and therapeutic potential of Cassia senna against prostate cancer in Wistar albino rats. Discover Applied Sciences. 2025; 7:1206.

[5] Natarajan SR, Krishnamoorthy R, Alshuniaber MA, Gatasheh MK, Rajagopal P, Veeraraghavan VP, Palanisamy CP, Jayaraman S. KDM1A Facilitates Oncogenic Potential in Colorectal Cancer Progression Through the Activation of AXIN/GSK3β/β-Catenin Signaling Pathways: Evidence From Integrated Transcriptomics and In Vitro Studies. The Journal of Gene Medicine. 2025; 27(11): e70053.

[6] Guan T, Gong J, Lin J, Palanisamy CP, Jinjin Pei J, El-Aty AMA. Machine learning-driven multimodal optimization of selenium biotransformation and flavor profiling in fermented apple–Yacon functional beverages. Innovative Food Science & Emerging Technologies. 2025; 105: 104198.

[7] Natarajan SR, Krishnamoorthy R, Alshuniaber MA, Alsulami TS, Gatasheh MK, Rajagopal P, Palanisamy CP, Govindan R, Veeraraghavan VP, Jayaraman S. ABCE1 facilitates tumour progression via aerobic glycolysis and inhibits cell death in human colorectal cancer cells through the p53 signalling pathway. Scientific Reports. 2025; 15: 24674.

[8] Huang Y, Guo H, Liu Y, Jin W, Palanisamy CP, Pei J, Oz F, El-Aty AMA. Effects of Natural Polysaccharides on the Gut Microbiota Related to Human Metabolic Health. Molecular Nutrition & Food Research. 2025; 69:e202400792.

[9] Poornima K, Meenakshi K.C, Manikandan V.R, Shankari G, Prabhu D, Rathi M.A, Palanisamy CP, Balaji R, Gopalakrishnan V.K. Exploring the anticancer potential of Jerantinine A from *Tabernaemontana coronaria* against prostate, breast, and ovarian cancers: A computational approach. *Journal of Complementary and Integrative Medicine*, 2025 22(2): 363–372.

[10] Palanisamy CP, Poompradub S, Sansanaphongpricha K, Jayaraman S, Subramani K. Faridah Sonsudin gGreen synthesis of Nigella sativa-mediated silver nanoparticles for enhanced antibacterial activity and wound healing: Mechanistic insights and biomedical applications. Environmental Nanotechnology, Monitoring & Management. 2025; 24: 101085.

[11] Surendran N, Raju MV, Chandrasekaran MK, Ahalliya RM, Palanisamy CP, Chandrasekaran G, Kanniappan GV. Physicochemical characterization of starch from Maranta arundinacea L.(arrowroot) rhizomes and its inhibition of COX-2: In vivo validation. Bioactive Carbohydrates and Dietary Fibre. 2025; 33: 100465.

[12] Kannappan P, Chandrasekaran MK, Raju MV, Gopalakrishnan S, Dhamodharan P, Ahalliya RM, Palanisamy CP, Raju B, Kanniappan GV. Exploring the anticancer potential of Jerantinine A from Tabernaemontana coronaria against prostate, breast, and ovarian cancers: a computational approach. Journal of Complementary and Integrative Medicine. 2025; 22(02): 363-372.

[13] Pei J, Kumarasamy RV, Jayaraman S, Kanniappan GV, Long Q, Palanisamy CP. Quercetin-functionalized nanomaterials: Innovative therapeutic avenues for Alzheimer's disease management. Ageing Research Reviews. 2025; 104: 102665.

[14] Jayaraman S, Prasad M, Natarajan SR, Krishnamoorthy R, Alshuniaber MA, Gatasheh MK, Veeraraghavan VP, Rajagopal P, Palanisamy CP. Molecular mechanisms underlying the effects of beta-sitosterol on TGF-β1/Nrf2/SIRT1/p53-mediated signaling in the kidney of a high-fat diet and sucrose-induced type-2 diabetic rat. Chemico-Biological Interactions. 2025; 411: 111443.

[15] Huang Y, Guo H, Liu Y, Jin W, Palanisamy CP, Pei J, Oz F, El-Aty AMA. Effects of Natural Polysaccharides on the Gut Microbiota Related to Human Metabolic Health. Molecular Nutrition & Food Research. 2025; e202400792.

[16] Prabhakaran P, Palanisamy CP, Shanmugam A, Damodharan P, Swaminathan H, Devaraj D, Ahalliya RM, Kanniappan GV. Isolation, structural characterization, and molecular docking studies on the bioactive compound from n-Hexane extract of Emilia sonchifolia (L.) DC against the pancreatic cancer target Aurora 2 Kinase. Journal of Complementary and Integrative Medicine. 2024; 22(1): 0290.

[17] Jiang H, Kumarasamy RV, Pei J, Raju K, Kanniappan GV, Palanisamy CP. Integrating engineered nanomaterials with extracellular vesicles: Advancing targeted drug delivery and biomedical applications. Frontiers in Nanotechnology. 2024; 6: 1513683.
[18] Guo H, Liu Y, Wan T, Song D, Palanisamy CP, Geng J, Pei J, Özmen S, El-Aty AMA. Toward personalized cancer management: Role of precision nutrition–diet interventions. Journal of Functional Foods. 2024; 123: 106584.
[19] Natarajan SR, Krishnamoorthy R, Alshuniaber MA, Al-Anazi KM, Farah MA, Rajagopal P, Palanisamy CP, Veeraraghavan VP, Jayaraman S. Identification of FOXM1 as a novel protein biomarker and therapeutic target for colorectal cancer progression: Evidence from immune infiltration and bioinformatic analyses. International Journal of Biological Macromolecules. 282 (Part 4): 137201.
[20] Perumal MKK, Renuka RR, Subbiah SK, Natarajan PM. Artificial intelligence-driven clinical decision support systems for early detection and precision therapy in oral cancer: a mini review. Frontiers in Oral Health. 2025; 6: 1592428.
[21] Ramesh E, Ganesan A, Lakshmi KC, Natarajan PM. Artificial intelligence-based diagnosis of oral leukoplakia using deep convolutional neural networks Xception and MobileNet-v2. Frontiers in Oral Health. 2025; 6: 1414524.
[22] Ganesan A, Kumar NG, Natarajan PM. Anticancer activity of silver nanoparticles synthesized from aqueous leaf extract of Solanum trilobatum (Purple fruit pea eggplant) on human oral cancer cells. Journal of Herbmed Pharmacololgy. 2024; 13(2): 260-268.
[23] Umapathy V, Dhanavel A, Kesavan R, Natarajan PM, Bhuminathan S, Vijayalakshmi P. Anticancer Potential of the Principal Constituent of Piper nigrum, Piperine: A Comprehensive Review. Cureus. 2024; 16(2): e54425.
[24] Umapathy VR, Swamikannu B, Natarajan PM, Devi R, Nandini MS, Vimalarani, Vijayalakshmi P. In Silico Molecular Docking of Ocimum sanctum Phytochemicals: Targeting Key Biomarkers in Oral Cancer. Journal of Pharmacy and Bioallied Sciences. 2024; 16(5): S4792-S4799.
[25] Swamikannu B, Umapathy VR, Natarajan PM, Nandini MS, Stylin AGSQ, Vimalarani V, Rajinikanth S. Unlocking the Therapeutic Benefits of Artemisia Annua: A Comprehensive Overview of its Medicinal Properties. Journal of Pharmacy and Bioallied Sciences. 2024; 16(5): S4248-S4253.
[26] Yadalam PK, Arumuganainar D, Natarajan PM, Ardila CM. Artificial intelligence-powered prediction of AIM-2 inflammasome sequences using transformers and graph attention networks in periodontal inflammation. Scientific Reports. 2025; 15: 8733.
[27] Yadalam PK, Chatterjee S, Natarajan PM, Ardila CM. Comparison of light gradient boosting and logistic regression for interactomic hub genes in Porphyromonas gingivalis and Fusobacterium nucleatum-induc ed periodontitis with Alzheimer's disease. Frontiers in Oral Health. 2025; 6:1463458.
[28] Yadalam PK, Natarajan PM, Ardila CM. Variational graph autoencoder for reconstructed transcriptomic data associated with NLRP3 mediated pyroptosis in periodontitis. Scientific Reports. 2025; 15: 1962.
[29] Daniel Raja FS, Abraham L, Rangasamy K, Saikia K, Rathankumar AK, Mironescu M, Mironescu I, Palanisamy CP, Kanniappan GV. Next-Generation Microbiome Therapeutics: Psychobiotics and Fecal Microbiota Transplants (FMT) for Mental Health Treatment. Frontiers in Cellular and Infection Microbiology. 2026; 16: 1719357.
[30] Dharmaprakash S, Gunasekaran VP, Sivaramakrishnan R, Kanniappan GV, Jayaraman S, Mironescu M, Rajabathar JR, Mironescu ID, Palanisamy CP. Marine macroalgae-mediated ultrasonic-assisted green synthesis of CuO nanoparticles embedded in starch/PVA electrospun nanoscaffolds for in vitro α-amylase and α-glucosidase inhibitory activity. Scientific Reports. 2026.
[31] Surendran N, Chandrasekaran G, Raju MV, Chandrasekaran MK, Ahalliya RM, Palanisamy CP, Kanniappan GV, Arcot R, Alharbi NS, Thiruvengadam M. Anti-inflammatory potential of ethanolic extract of Maranta arundinacea L.: Insights from COX-2 modulation and oxidative stress analysis. South African Journal of Botany. 2026; 195: 142-151.
[32] Pei J, Senthilkumar MV, Hessini K, Subramaniyam S, Sivaramakrishnan R, Kanniappan GV, Jayaraman S, Palanisamy CP. Green fabrication of starch/PVA/CuO nanoscaffolds using marine macroalgae extract for enhanced anti-inflammatory activity. Sustainable Chemistry and Pharmacy. 2026; 51: 102397.
[33] Balasubramanian V, Loganathan L, Muthuswamy K, Viswanathan TM, Raju MV, Chandrasekaran MK, Ahalliya RM, Poorasamy J, Palanisamy CP, Dominic S, Kanniappan GV. Anticancer therapeutic efficacy of PEGylated β-galactosidase from Aspergillus terreus in DMBA-induced breast cancer: Toxicological, molecular and histopathological evaluation in Wistar rats. International Journal of Biological Macromolecules. 2026; 360: 151856.
[34] Jayaraman S, Eswaran A, Rajagopal P, Palanisamy CP, Veerakumar P, Veeraraghavan VP, Sirasanagandla SR. Neuroendocrine-associated epigenetic factors in cellular senescence: mechanisms and therapeutic implications. Biogerontology. 2026; 27(2): 64.

[35] Ponnusamy B, Rajagopal P, Palanisamy CP, Veeraraghavan VP, Jayaraman S. Mechanistic Exploration of the anticancer activity of Justicia adhatoda Plant Leaf Ethanolic Extract against Colon Cancer Cells: An in silico and in vitro Approach. Asian Pacific Journal of Cancer Prevention. 2026; 27(3): 1069-1080.
[36] Pei J, Saran VS, Sivaramakrishnan R, Kanniappan GV, Pandurangan V, Jayaraman S, Dhayalan VK, Mironescu M, Mironescu ID, Palanisamy CP. Ultrasonic-assisted, Sargassum ilicifolium (brown marine macroalgae)-mediated biogenic synthesis of CuO nanoparticles incorporated in starch/PVA electrospun nanoscaffolds: In vitro safety and antioxidant efficacy assessment. Bioorganic Chemistry. 2026; 173: 109679.
[37] Raj MAPA, Subramaniyam S, Kanniappan GV, Jayaraman S, Palanisamy CP. Sustainable fabrication of starch/PVA/CuO electrospun nanoscaffolds from Turbinaria ornata (marine macroalgae) extract: Physicochemical characterization and antidiabetic evaluation. Kuwait Journal of Science. 2026; 53(2): 100545.
[38] Pei J, Ganesh NS, Subramaniyam S, Sivaramakrishnan R, Kanniappan GV, Jayaraman S, Palanisamy CP. Sustainable fabrication of starch/PVA/CuO electrospun nanoscaffolds from Padina tetrastromatica (Brown macroalgae) extract: Physicochemical characterization and antidiabetic assessment. Sustainable Chemistry One World. 2026; 9: 100195.
[39] Sakthiraj A, Sivaramakrishnan R, Subramaniyam S, Kanniappan GV, Pandurangan V, Jayaraman S, Dhayalan VK, Mironescu M, Mironescu ID, Palanisamy CP. Starch/PVA electrospun nanoscaffolds loaded with ultrasonic-assisted green-synthesis of CuO nanoparticles from marine macroalgae (Gracilaria corticata) extract: Cytotoxicity and antioxidant analysis. Chemical Physics Impact. 2026; 12: 101018.
[40] Raju M, Chandrasekaran MK, Loganathan L, Ahalliya RM, Mironescu M, Mironescu ID, Palanisamy CP, Kanniappan GV. Lipid remodeling and ferroptosis in phosphatidylcholine-mediated tumor–stroma crosstalk. Frontiers in Molecular Biosciences. 2026; 13: 1742305.
[41] Kunamalla R, Panagal M, Palanisamy CP. Biogenic synthesis and fabrication of starch/PVA/CuO electrospun nanoscaffolds from Sargassum ilicifolium (brown marine macroalgae) extract for anticancer activity on HT-29 and MCF-7 cancer cells. Biocatalysis and Agricultural Biotechnology. 2026; 72: 103923.
[42] Pei J, Govindaraj H, Sivaramakrishnan R, Kanniappan GV, Pandurangan V, Dhayalan VK, Mironescu M, Mironescu ID, Jayaraman S, Palanisamy PC. Sustainable fabrication of biopolymer-based (starch/PVA) nanoscaffolds loaded with green-synthesized CuO nanoparticles from Sargassum wightii (marine macroalgae): Cytocompatibility and antioxidant activity. Biomaterials Advances. 2026; 182: 214660.
[43] Pei J, Perumal NC, Meng P, Long Q, Palanisamy CP. Extracellular vesicle-based biosensors for Alzheimer's disease: A new frontier in precision diagnostics. Ageing Research Reviews. 2026; 113: 102904.
[44] Natarajan PM. Dental Bioinformnatics-Current Scope and Future perspectives. Research Journal of Pharmacy and Technology. 2022;15(5):2351-6.
[45] Natarajan PM, Umapathy VR, Murali A, Swamikannu B. (2022). Computational Simulations of Identified marine-derived Natural Bioactive Compounds As Potential Inhibitors of Oral Cancer. Future Science OA. 2022; 8(3).
[46] Natarajan PM, Umapathy VR. Role of transcriptomics in the study of oral cancer. Frontiers in Oral Health. 2025; 6:1524364.
[47] Natarajan PM, Swamikannu B, Sivaraman NM, Stylin AGSQ. Prevention of Oral Cancer: A Comprehensive Guide. Journal of Pharmacy and Bioallied Sciences. 2024; 16(5): S4239-S4241.
[48] Natarajan PM. Computational Studies on Recent Congeners of Fluoroquinolones and Nitroimidazoles for Their Use in Periodontal Therapy. Journal of Pharmacy and Bioallied Sciences. 2024; 16(5): S4731-S4740.
[49] Natarajan PM, Bhuminathan S, Rajan R, Bindu K, Loganathan K, Veerakumar R. The Crucial Role of Smoking Cessation in Preventing Oral Cancer. Journal of Pharmacy and Bioallied Sciences. 2024; 16(5): S4245-S4247.
[50] Natarajan PM, Bhuminathan S, Leela B, Bindu K, Loganathan K, Ramachandran V. Smoking and its Role in Oral Cancer. Journal of Pharmacy and Bioallied Sciences 16(5): S4242-S4244.
[51] Vidhyarekha U, Natarajan PM, Bhuminathan S, Sabarinathan J, Suba R, Vijayalakshmi P. Role of artificial intelligence in Oral Cancer. Advances in Public Health. 2024. 2024: 3664408.
[52] Ganesan A, Kumar NG, Natarajan PM, Gauthaman J. Automated classification of elongated styloid processes using deep learning models-an artificial intelligence diagnostics. Frontiers in Oral Health. 2025; 5: 1424840.
[53] Umapathy VR, Natarajan PM, Swamikannu B. Regenerative Strategies in Dentistry: Harnessing Stem Cells, Biomaterials and Bioactive Materials for Tissue Repair. Biomolecules. 2025; 15: 546.
[54] Ganesan A, Kumar NG, Natarajan PM. Solanum trilobatum leaf extract-derived silver nanoparticles downregulate the PI3K/AKT/mTOR signaling pathway and attenuate oral squamous cell carcinoma cell proliferation. Journal of Herbmed Pharmacology. 2024; 13(2): 300-307.
[55] Rajendran MS, Jayaraman S, Khan JM, Jasmine S, Prabhakaran RK, Raju MV, Chandrasekaran MK, Ahalliya RM, Kannappan P, Palanisamy CP, Kanniappan GV. Investigating the colon toxicity and carcinogenic role of monosodium glutamate compared with Dimethylhydrazine in male Wistar rats:

Exploring the link to childhood colon cancer risk. Journal of King Saud University - Science. 2024; 36(11): 103507.
[56] Kumarasamy RV, Natarajan P, Umapathy VR, Roy JR, Rab SO, Saeed M, Panagal M, Mironescu M, Srinivasan GP, Palanisamy CP. Clinical Applications and Therapeutic Potentials of Advanced Nanoparticles: A Comprehensive Review on Completed Human Clinical Trials. Frontiers in Nanotechnology. 2024; 6:1479993.
[57] Jin W, Pei JJ, Roy JR, Jayaraman S, Ahalliya RM, Kanniappan GV, Mironescu M, Palanisamy CP. Comprehensive review on single-cell RNA sequencing: A new frontier in Alzheimer's disease research. Ageing Research Reviews. 2024; 274: 102454.
[58] Pei J, Palanisamy CP, Jayaraman S, Natarajan PM, Umapathy VR, Roy JR, Panagal M, Jayaraman S. Curcumin-loaded polymeric nanomaterials as a novel therapeutic strategy for Alzheimer's disease: A comprehensive review. Ageing Research Reviews. 2024; 99: 102393.
[59] Pei J, Palanisamy CP, Jayaraman S, Natarajan PM, Umapathy VR, Roy JR, Thalamati D, Ahalliya RM, Kanniappan GV, Mironescu M. A comprehensive review on starch-based Sustainable Edible Films Loaded with Bioactive Components for Food Packaging. International Journal of Biological macromolecules. 2024; 274 (Part-1): 133332.
[60] Palanisamy CP, poompradub S, Sansanaphongpricha K, Subramani K, Sonsudin F. Increased expression levels of PDGF and VEGF magnify the wound healing potential facilitated by biogenic synthesis of silver nanoparticles. Nano-Structures & Nano-Objects. 2024; 39: 101236.
[61] Pei J, Palanisamy CP, Jayaraman S, Natarajan PM, Umapathy VR, Roy JR, Thalamati D, Ahalliya RM, Kanniappan GV, Mironescu M. Proteomics Profiling of Extracellular Vesicle for Identification of Potential Biomarkers in Alzheimer's Disease: A Comprehensive Review. Ageing Research Reviews. 2024; 99: 102359.
[62] Xi J, Wang T, Xian P, Liu X, Du M, Yang H, Palanisamy CP, Lin W, Long Q. Proteomic insights uncover enhanced neurotherapeutic potential in conditioned mesenchymal stem cell-derived extracellular vesicles. Extracellular Vesicle. 2024; 3: 100037.
[63] Pei J, Natarajan PM, Umapathy VR, Swamikannu B, Sivaraman NM, Krishnasamy L, Palanisamy CP. Advancements in the synthesis and functionalization of zinc oxide-based nanomaterials for enhanced oral cancer therapy. Molecules. 2024; 29(11): 2706.
[64] Gatasheh MK, Natarajan SR, Krishnamoorthy R, Alsulami TS, Rajagopal P, Palanisamy CP, Veeraraghavan VP, Jayaraman S. Molecular analysis to identify novel potential biomarkers as drug targets in colorectal cancer therapy: an integrated bioinformatics analysis. Molecular and Cellular Oncology. 2024; 11(1): 2326699.
[65] Pei J, Yan Y, Jayaraman S, Rajagopal P, Natarajan PM, Umapathy VR, Gopathy S, Roy JR, Sadagopan CS, Thalamati D, Palanisamy CP, Mironescu M. A review on advancements in the application of starch-based nanomaterials in biomedicine: Precision drug delivery and cancer therapy. International Journal of Biological Macromolecules. 2024; 130746.
[66] Pei JJ, Yan Y, Palanisamy CP, Jayaraman S, Natarajan PM, Umapathy VR, Gopathy S, Roy JR, Sadagopan JC, Thalamati D, Mironescu M. Materials-based drug delivery approaches: Recent advances and future perspectives. Green Processing and Synthesis. 2024; 13: 20230094.
[67] Pei JJ, Deng W, Liu Y, Guo Y, Chen J, Abdu H, Khan MR, Palanisamy CP, El-Aty AM. A Comprehensive Review of Cornus officinalis: Health Benefits, Phytochemistry, and Pharmacological Effects for Functional Drug and Food Development. Frontiers in Nutrition. 2023; 10: 1309963.
[68] Alugoju P, Palanisamy CP, Anthikapalli NVA, Jayaraman S, Prasanskulab A, Chuchawankul S, Dyavaiah M, Tencomnao T. Exploring the anti-aging potential of natural products and plant extracts in budding yeast Saccharomyces cerevisiae: A review. F1000Research. 2023; 12: 1265.
[69] Lavanya M, Krishnamoorthy R, Alshuniaber MA, Manoharadas S, Palanisamy CP, Veeraraghavan VP, Jayaraman S, Rajagopal P, Padmini R. Formulation, characterization and evaluation of gelatin-syringic acid/zinc oxide nanocomposite for its effective anticancer, antioxidant and anti-inflammatory activities. Journal of King Saud University-Science. 2023; 35: 102909.
[70] Palanisamy CP, Poompradub S, Sansanaphongpricha K, Jayaraman S, Subramani K, Sonsudin F. Biosynthesis of silver nanoparticles (AgNPs) using ethanolic extract of Nigella sativa (L.) seeds promotes wound healing via PDGF and VEGF signalling pathways activation. Biocatalysis and Agricultural Biotechnology. 2023; 54: 102970.